LEAF SPECTRAL TYPES, RESIDUALS, AND CANOPY SHADE IN AN AVIRIS IMAGE

Roberts, D.A., Smith, M.O., Adams, J.B. and Gillespie, A.R.
Department of Geological Sciences
University of Washington
Seattle, Washington

INTRODUCTION

Spectral mixture analysis was applied to AVIRIS data collected over Jasper Ridge, CA on September 20, 1989. The analysis focused on non-linear spectral mixing between green vegetation and soils and the separation of non-green vegetation, vegetation types and soils using linear spectral mixture analysis and residual analysis (Smith et al., 1987; Gillespie et al., 1990; Roberts et al., 1990; Sabol et al., 1991).

METHODS

The basic linear-spectral mixing model is shown in equation 1.

$$DN_i = g_i \sum_{j=1}^{n} f_j * \rho_{ij} + o_i + \varepsilon_i \quad [1]$$

Using this equation encoded radiance at band i, DN_i, is modeled as the sum of n laboratory reflectance endmembers, ρ_{ij}, each weighted by the fraction of the material in the field of view, f_j. Multiplicative and additive factors used to calibrate encoded radiance to reflectance are shown as g_i, and o_i, respectively. ε_i is a residual term that accounts for all spectral variability that is not accounted for by mixtures of the endmembers and the calibration terms.

Our objective when employing linear spectral mixture analysis was to locate the minimum number of endmembers that described the greatest amount of spectral variability within the scene. To locate other materials, which were not explicitly modeled using endmember spectra we analyzed residual spectra (Equation 2):

$$\varepsilon_i = DN_i - g_i \sum_{j=1}^{n} f_j * \rho_{ij} + o_i \quad [2]$$

Residual spectra can be used to identify materials based on wavelength-dependent positive or negative residuals.

Non-linear spectral mixing occurs when one or more spectra that comprise a mixture contribute more or less to the mixture than should occur based on the proportion of materials in the field of view. Non-linear spectral mixing has been shown to occur between intimate mineral mixtures (e.g. Nash and Conel, 1974; Johnson et al., 1983). Recently it has been shown to also occur between green vegetation and soils (Roberts et al., 1990b, Roberts 1991). Non-linear spectral mixing between green vegetation and soils is primarily a product of the transmission/scattering of NIR light by green vegetation. Roberts (1990a), using

numerical simulations found that a linear mixing model, when applied to mixtures of green vegetation, soils and shade overestimated the green-leaf fraction and underestimated the shade fraction. To determine whether non-linear spectral mixing was significant in AVIRIS data, linear spectral mixing analysis was applied separately to three wavelength regions, the visible, near-infrared (NIR) and short-wave-infrared (SWIR). This approach was used as a test of non-linearity, which should be expressed as different fractional estimates of green-vegetation and shade in the visible, NIR and SWIR subsets. Based on the numerical models, we predicted that the green-leaf fraction estimated from the NIR spectral subset would be higher than the estimates using the visible spectral subset.

A new method was developed to derive improved estimates of green-leaf and shade fractions from non-linear spectral mixtures. This approach was based on the derivation of a canopy shade spectrum (Equation 3).

$$S_\lambda = (P_\lambda - f_l * \rho_{l\lambda})/f_s \quad [3]$$

Canopy shade, S_λ, was calculated by subtracting a green-leaf spectrum, $\rho_{l\lambda}$, weighted by the fraction of green-leaf, f_l, from the measured/calibrated encoded radiance spectrum, P_λ, and dividing the difference by the fraction of shade, f_s. Using this approach canopy shade spectra was generated for each combination of green-leaf and shade fractions. By constraining the spectrum of shade to be near zero in red light and positive in the NIR a new set of estimates for green-leaf and shade was derived.

When a scene contains more endmembers than green-leaf and shade, equation 3 can be generalized to:

$$S_\lambda = (P_\lambda - \sum_{i=1}^{n-1} f_i * \rho_{i\lambda})/f_s \quad [4]$$

RESULTS

The data were calibrated to reflectance using two techniques, an empirical line calibration (Roberts et al., 1986; Elvidge and Portigal, 1990; Conel, 1990) and the linear mixing approach (Smith et al., 1987). We found that non-linear spectral mixing between green vegetation, soils and shade adversely affected the mixing-model calibration when green vegetation was included as an endmember. In canopies, this non-linearity was expressed as a canopy shade spectrum that differed from the photometric (spectrally flat) shade used for calibration. Resulting calibration factors (g_λ and o_λ) derived from the linear-mixing model produced reflectance spectra that had unreasonably high visible reflectance relative to NIR reflectance (Figure 1). The empirical line calibration was not affected by non-linearities only because vegetation was not employed as a calibration target. Under similar conditions the mixing model calibration will be comparable.

Most of the spectral variability in the image was described by three reference spectra (endmembers): green vegetation, soil and shade. Additional endmembers produced an unstable solution of the mixing equation, degrading the fractional estimates. Other materials known to occur in the image were located by analysis of residual spectra (Figure 2). Using this approach we found that senescent grass could be distinguished from soils based on negative residuals centered at 2100 and 2300 nm.

Negative residuals at 2100 and 2300 nm resulted from absorption by cellulose and lignin in the plant material. Residual analysis was also employed to map soils. Four soils were mapped based on residuals. These included a soil that produced a negative residual centered at 2207 nm, attributed to clay, one that produced a negative residual centered at 1042 nm and one that produced negative residuals at wavelengths shorter than 850 nm (e.g. J9009176 on Figure 2), probably due to ferric iron. The fourth soil corresponded to the soil endmember in the analysis.

Residual spectra were also found to be highly sensitive to spatial/elevational variability in atmospheric attenuation and backscattering. Reduced atmospheric attenuation at higher elevations than the calibration sites was expressed as positive residuals within the atmospheric water bands (Positive spikes in Figure 2). Increased atmospheric backscattering was observed on the eastern half of the image. Atmospheric backscattering did not detract greatly from analysis of the residuals but did have a severe affect on the linear models of the visible spectral subset.

Linear mixing models of the visible, NIR and SWIR spectral subsets demonstrated good correspondence with the numerical predictions for non-linearity. As predicted, green-leaf fractions estimated from the NIR spectral subset were significantly higher than those estimated from the visible spectral subset. Linear models of the visible, NIR and SWIR spectral subsets proved to be useful for distinguishing different types of vegetation, as well as for demonstrating non-linear spectral mixing. Spectrally distinct vegetation types, which could neither be treated as separate endmembers nor distinguished using residual spectra, produced different green-leaf fractions in the three spectral subsets (Figure 3). Two areas were examined in detail. One of the areas, a golf course, produced high green-leaf fractions in all three spectral subsets, suggesting that the dominant vegetation in the area has high visible, high NIR and high SWIR reflectance. This result matches the known spectral properties of leaves in the area. The other area, a forested wetland, produced low green-leaf fractions in the visible and SWIR subsets and high fractions in the NIR suggesting that the dominant vegetation has low visible and SWIR reflectance and high NIR reflectance. Once again, the results matched the known spectral properties of leaves in the area.

Improved estimates of the fraction of green leaf and shade were derived by solving for canopy shade (Figures 4 and 5). Using this approach new shade estimates were derived for the the forested wetland (Swamp) and the golf course vegetation (Lawn). The new estimates for shade were significantly higher than estimates derived from the linear-mixing model. Furthermore, it was found that the canopy shade spectrum derived using this approach was related to vegetation types, varying depending on the transmittance of leaves in the canopy and the architecture of the canopy.

REFERENCES

Conel, J.E., 1990, Determination of Surface Reflectance and Estimates of Atmospheric Optical Depth and Single Scattering Albedo from Landsat Thematic Mapper Data, *Int. J. Remote Sensing*, 11(5): 783-828.

Elvidge, C.D., and Portigal, F.P., 1990, Change Detection in Vegetation using 1989 AVIRIS data, Proc. SPIE Imaging Spectroscopy of the Terrestrial Environment, (G. Vane ed.), Orlando, FL, April 16 - 17, 1990, p. 178-189.

Gillespie, A.R., Smith, M.O., Adams, J.B., Willis, S.C., Fischer, A.F., and Sabol, D.E., 1990, Interpretation of Residual Images: Spectral Mixture Analysis of AVIRIS Images, Owens Valley, California, Proc. 2nd Airborne Visible/Infrared Imaging Spectrometer (AVIRIS) Workshop, Pasadena, Ca, June 4-5, 1990, (R.O. Green, ed.), JPL Publication 90-54, pp.243-270.

Johnson, P.E., Smith, M.O., Taylor-George, S., and Adams, J.B., 1983, A Semiempirical Method of Analysis of the Reflectance Spectra of Binary Mineral Mixtures, *J. Geophys. Res.*, 88: 3557-3561.

Nash, D.B., and Conel, J.E., 1974, Spectral Reflectance Systematics for Mixtures of Powdered Hypersthene, Labradorite, and Ilmenite, *J. Geophys. Res.*, 79(11): 1615-1621.

Roberts, D.A., 1991, Separating Spectral Mixtures of Vegetation and Soils, Unpublished Ph.D. Dissertation, University of Washington.

Roberts, D.A., Adams, J.B., and Smith, M.O., 1990a, Transmission and Scattering of Light by Leaves: Effects on Spectral Mixtures, Proc. IGARRS, College Park, Md, May 20-24, 1990, pp. 1381`-1385.

Roberts, D.A., Smith, M.O., Adams, J.B., Sabol, D.E., Gillespie, A.R., and Willis, S.C., 1990b, Isolating Woody Plant Material and Senescent Vegetation From Green Vegetation in AVIRIS Data, Proc. 2nd Airborne Visible/Infrared Imaging Spectrometer (AVIRIS) Workshop, Pasadena, Ca, June 4-5, 1990, (R.O. Green, ed.), JPL Publication 90-54, pp. 243-270.

Roberts, D.A., Yamaguchi, Y., and Lyon, R.J.P., 1986, Comparison of Various Techniques for Celebration of AIS Data, Proc. 2nd Airborne Imaging Spectrometer Data Analysis Workshop, May 6-8, 1986, JPL Publication 86-35, pp. 243-270.

Sabol, D.E., Adams, J.B., Smith, M.O., and Gillespie, A.R., 1991, Target Detection Thresholds Using Imaging Spectrometer Data, Proc. 3rd Airborne Visible/Infrared Imaging Spectrometer (AVIRIS) Workshop, Pasadena, Ca, May 20-21, 1991, (R.O. Green, ed.), JPL Publication 91-28 (this publication).

Smith, M.O., Roberts, D.A., Shipman, H.M., Adams, J.B., Willis, S.C., and Gillespie, A.R., 1987, Calibrating AIS Images Using the Surface as a Reference, Proc. 3rd Airborne Imaging Spectrometer Data Analysis Workshop, June 2-4, 1987, JPL Publication 87-30, 10 pp.

ACKNOWLEDGEMENTS

We thank Steve Willis for his programming assistance. This research was supported by NASA grant NAGW 1319 and a grant from the W.M. Keck Foundation for computer equipment and support.

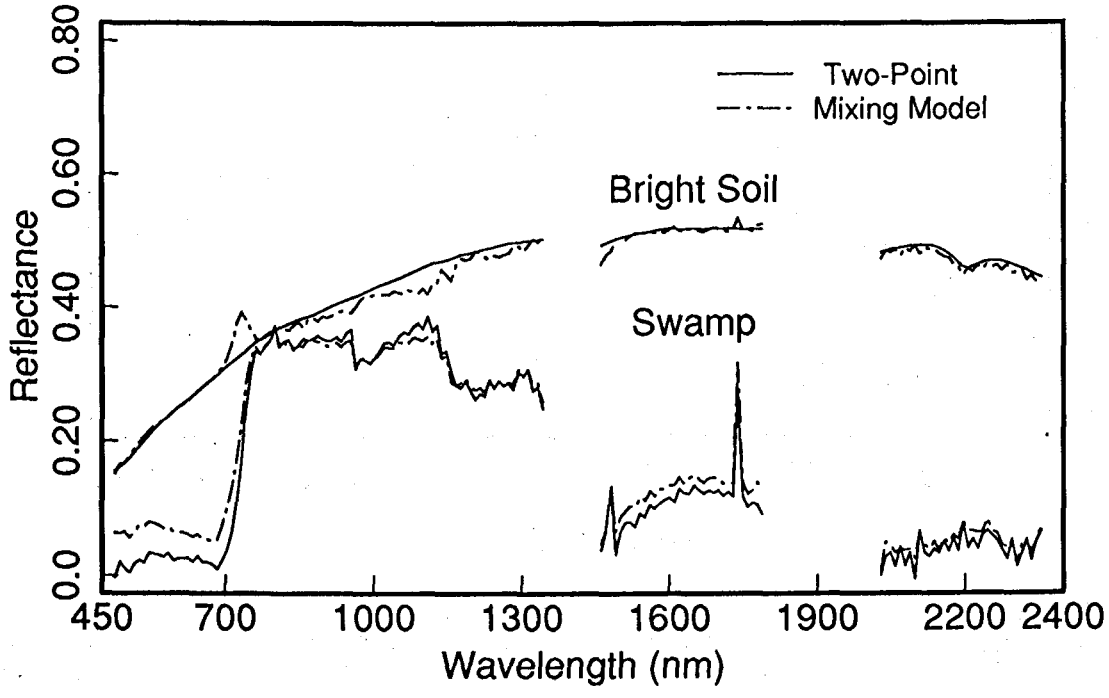

Figure 1. Comparison of the empirical line calibration using non-vegetated targets (two-point - solid) and the mixing model calibration using green vegetation as an endmember(dashed). Two of the calibration sites, Bright Soil and Swamp are shown. Note the similarity between the two results at wavelengths beyond 800 nm. At shorter wavelengths the mixing model calibration produced higher reflectance values than the empirical line calibration.

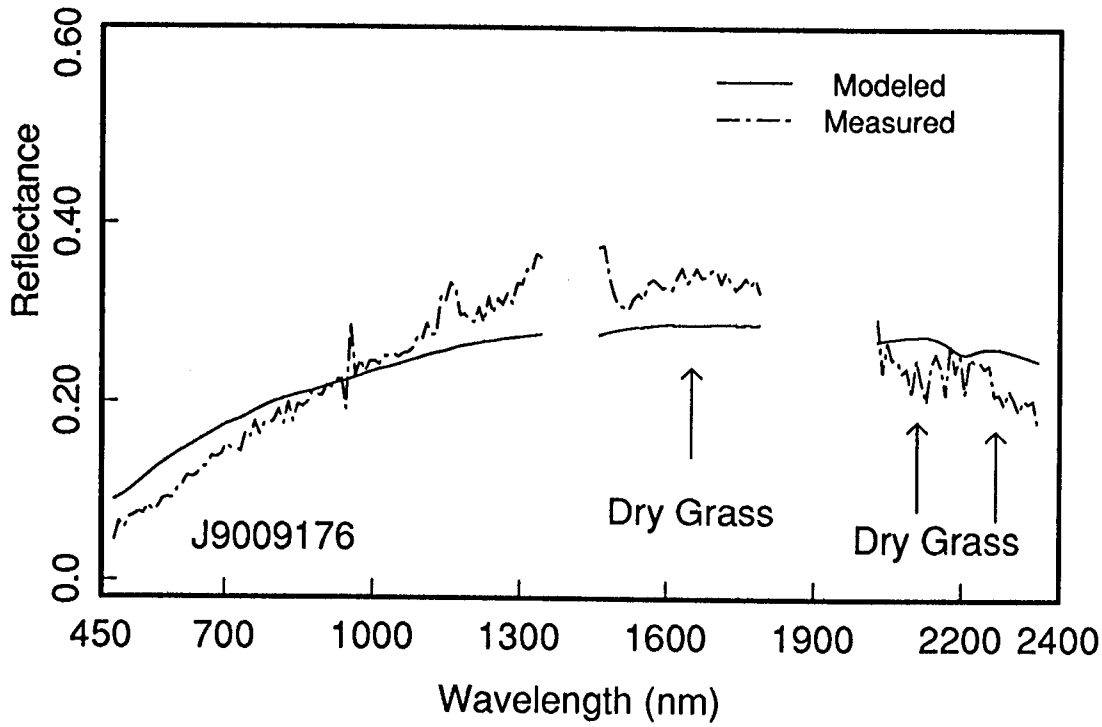

Figure 2. Modeled reflectance spectrum (solid) compared to a measured/ calibrated spectrum for an area dominated by senescent grass located on the central portion of Jasper Ridge. The modeled spectrum was calculated as the linear sum of fractions of green-leaf, shade and soil determined for the area using a linear mixing model. Cellulose and lignin in dry grass produce absorptions in the measured/calibrated spectrum at 2100 and 2300 nm. When a residual spectrum was calculated, the presence of these absorptions produced negative residuals. Negative residuals between 450 and 900 nm are a product of the background soil, which was spectrally distinct from the soil endmember used in the model. Positive features at 940, 1130 and 1400 nm are a product of reduced atmospheric attenuation with increased elevation (Green et al., 1990).

Figure 3. False color composite showing visible, NIR and SWIR green-leaf fractions estimated from the spectral subsets as red, green and blue, respectively. The most obvious feature is a pronounced west (right) to east (left) gradient from blue-green to red in the image. This gradient is a product of increased atmospheric backscattering towards the east, which is modeled as increased green-leaf fractions in the visible model (red). Different vegetation types produced different green-leaf fractions in the three wavelength regions. Grass in the golf courses appears white in the middle of the image, towards the top, due to high green-leaf fractions estimated in all three wavelength regions. Forested wetland (swamp - mid-right) appears green due to low green-leaf fractions in the visible and SWIR and a high green-leaf fraction in the NIR. In all cases, green-leaf fractions estimated using the NIR were higher than they were using visible light [see slide 4].

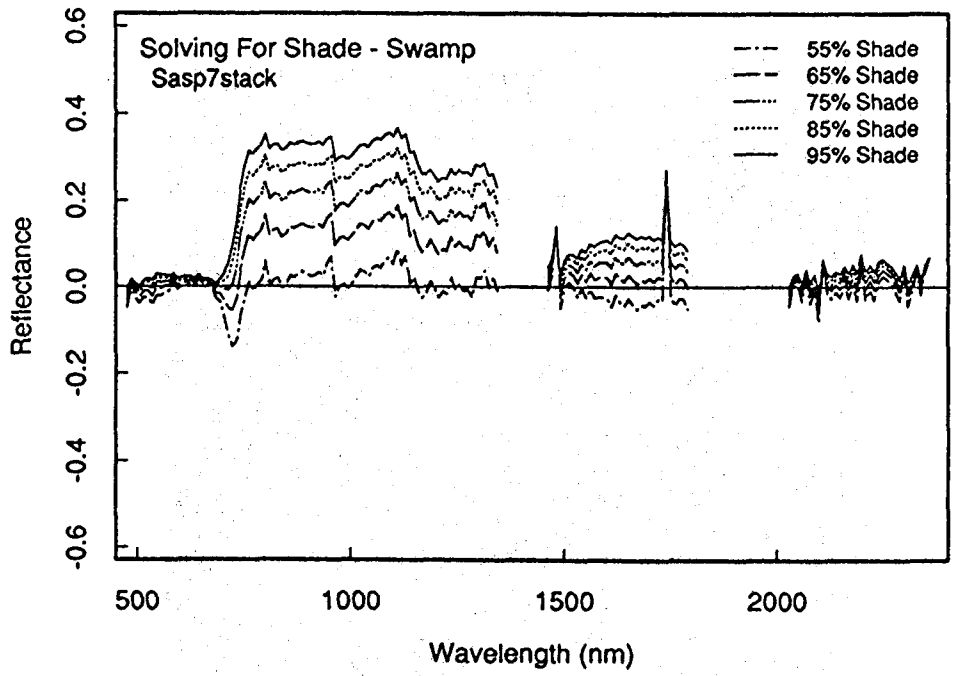

Figure 4. Canopy shade spectra for the forested wetland (Labeled swamp in the Figure). A reasonable shade spectrum was derived at a shade fraction of 85%. Linear estimates for this same area were 56% shade.

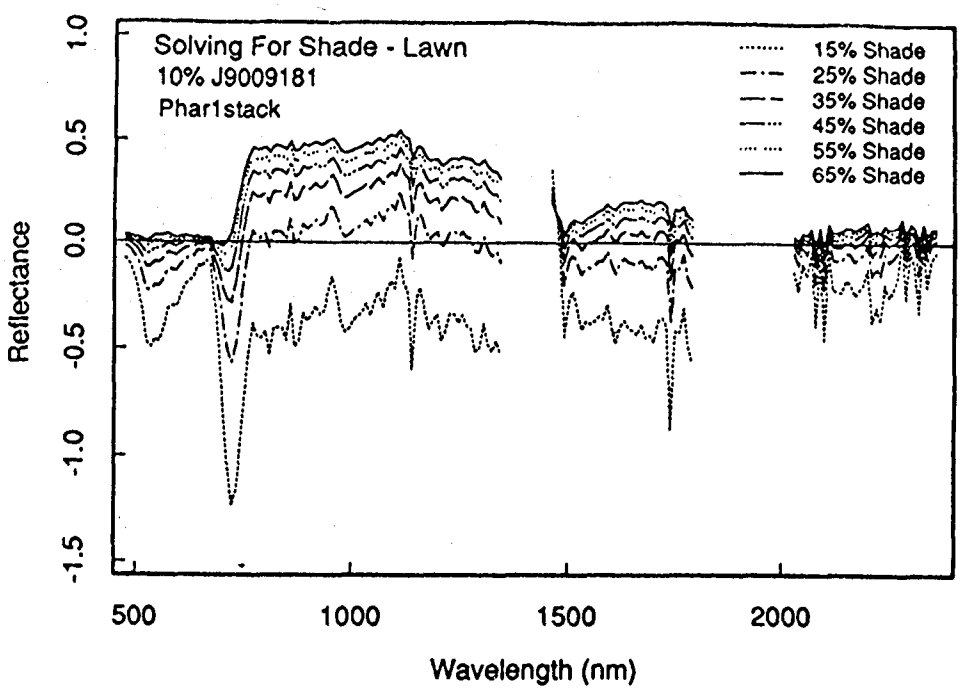

Figure 5. Canopy shade spectra for the golf course grass (Labeled lawn in figure). Shade fractions from this analysis were 65% compared to an estimate of 18% using the linear model. Compare the shade spectrum derived for the grass to the shade spectrum derived for the forested wetland (Figure 4). Note, shade fractions at the golf course were lower, yet the NIR "reflectance" of the shade was much higher.